Earth's Future

RESEARCH ARTICLE
10.1029/2022EF002685

Special Section:
Fire in the Earth System

Fire and Ice: The Impact of Wildfire-Affected Albedo and Irradiance on Glacier Melt

Caroline Aubry-Wake[1], André Bertoncini[1], and John W. Pomeroy[1]

[1]Centre for Hydrology, University of Saskatchewan, Canmore, AB, Canada

Key Points:

- The effect of wildfire smoke on the energy and mass balance of Athabasca Glacier, Canada was investigated using measurements and modeling
- Wildfire smoke reduced surface net irradiance, causing net radiation to decrease by 15 Wm^{-2} during smoky conditions
- In the years after record wildfires activity, the lowered albedo from antecedent soot deposition still increased ice melt by up to 10%

Supporting Information:

Supporting Information may be found in the online version of this article.

Correspondence to:

C. Aubry-Wake,
caroline.aubrywake@gmail.com

Citation:

Aubry-Wake, C., Bertoncini, A., & Pomeroy, J. W. (2022). Fire and ice: The impact of wildfire-affected albedo and irradiance on glacier melt. *Earth's Future*, *10*, e2022EF002685. https://doi.org/10.1029/2022EF002685

Received 21 JAN 2022
Accepted 30 MAR 2022

Author Contributions:

Conceptualization: Caroline Aubry-Wake, John W. Pomeroy
Data curation: Caroline Aubry-Wake
Formal analysis: Caroline Aubry-Wake, André Bertoncini
Funding acquisition: John W. Pomeroy
Investigation: Caroline Aubry-Wake
Methodology: Caroline Aubry-Wake, André Bertoncini, John W. Pomeroy
Project Administration: John W. Pomeroy

Abstract Wildfire occurrence and severity is predicted to increase in the upcoming decades with severe negative impacts on human societies. The impacts of upwind wildfire activity on glacier melt, a critical source of freshwater for downstream environments, were investigated through analysis of field and remote sensing observations and modeling experiments for the 2015–2020 melt seasons at the well-instrumented Athabasca Glacier in the Canadian Rockies. Upwind wildfire activity influenced surface glacier melt through both a decrease in the surface albedo from deposition of soot on the glacier and through the impact of smoke on atmospheric conditions above the glacier. Athabasca Glacier on-ice weather station observations show days with dense smoke were warmer than clear, non-smoky days, and sustained a reduction in surface shortwave irradiance of 103 W m^{-2} during peak shortwave irradiance and an increase in longwave irradiance of 10 W m^{-2}, producing an average 15 W m^{-2} decrease in net radiation. Albedo observed on-ice gradually decreased after the wildfires started, from a summer average of 0.29 in 2015 before the wildfires to as low as 0.16 in 2018 after extensive wildfires and remained low for two more melt seasons without substantial upwind wildfires. Reduced all-wave irradiance partly compensated for the increase in melt due to lowered albedo in those seasons when smoke was detected above Athabasca Glacier. In melt seasons without smoke, the suppressed albedo increased melt by slightly more than 10% compared to the simulations without fire-impacted albedo, increasing melt by 0.42 m. w.e. in 2019 and 0.37 m. w.e. in 2020.

Plain Language Summary Wildfire activity, which is expected to increase in the upcoming decades, has wide-ranging consequences. Wildfire smoke can drift to far mountains range and change the amount of glacier melt, an important source of water for downstream environments. On the Athabasca Glacier, in the Canadian Rockies, the impacts of wildfire smoke on glacier melt were investigated using weather measurements collected on the glacier and computer simulations for the 2015–2020 melt seasons. Smoky days were found to be warmer, drier and with lower incoming solar energy than days without smoke. During heavy fire years, the wildfire smoke deposited on the glacier surface gradually darkens the ice. The glacier surface stayed dark in the following years, even when no-fire activity was detected. This darker ice surface caused ice melt to increase by up to 10% compared to simulations where the impacts of fire activity were removed. However, in years when smoke was detected, the increased melt due to the darker ice surface was partially compensated by a reduction in how much solar energy reached the ice. This works helps us understand climate change, wildfires, and glacier melt are connected, and better predict future water resources in mountain regions.

1. Introduction

Human-induced climate change, causing warmer spring and summer temperatures and earlier snowmelt, is driving an increase in global forest fire occurrence (Gillett, 2004; Westerling et al., 2006). Predictions of future fire activity under climate change scenarios show an increase in extreme fire danger (Abatzoglou et al., 2019; Bedia et al., 2014; Kilpeläinen et al., 2010; Stocks et al., 2003). Forest fires have a wide-ranging impact on surrounding environments and human activities, impacting air quality, snowmelt and flooding (Burles & Boon, 2011; Gleason et al., 2019; Pomeroy et al., 2012; Versini et al., 2013).

Ongoing climate change is accelerating melt of the mountain cryosphere and threatening downstream water resources (Huss & Hock, 2018; Immerzeel et al., 2020). The net radiation received at the glacier surface controls this melt (Hock, 2005). Mountain snow and ice surfaces typically have high albedos and so reflect an extensive amount of solar radiation. However, forest fires upwind of snow and ice covers can affect the melt patterns through the deposition of light-absorbing impurities (LAI). Surface darkening due to LAI results in higher absorption of solar radiation and faster melt (Conway et al., 1996; Skiles et al., 2018; Warren & Wiscombe, 1980). Keegan

Supervision: John W. Pomeroy
Visualization: Caroline Aubry-Wake, André Bertoncini
Writing – original draft: Caroline Aubry-Wake
Writing – review & editing: Caroline Aubry-Wake, André Bertoncini, John W. Pomeroy

et al. (2014) linked widespread accelerated melt of the Greenland ice sheet to Northern Hemisphere forest fires, and more recently, Magalhães et al. (2019) have shown that forest fires in the Amazon are accelerating the melt of Andean glaciers. Williamson and Menounos (2021) have shown that mountain glacier albedo is declining across North America and the decline is correlated not only with rising temperature but also with forest fire LAI deposition. LAI deposition can feed microbial growth, triggering a feedback loop that further decreases the surface albedo (Cook et al., 2020; Di Mauro et al., 2020; Ryan et al., 2018). Besides darkening the surface, wildfire smoke reduces incoming shortwave radiation (McKendry et al., 2019; Sokolik et al., 2019; Stone et al., 2008) and can even lead to surface cooling (Kochanski et al., 2019). These two processes, the surface darkening because of LAIs, and the attenuation in incoming solar radiation because of the wildfire smoke, can therefore compensate each other. Even though this has been suggested in the literature (e.g., Stone et al., 2008), it has not previously been quantified.

The objective of this paper is to better understand the roles of several possible processes that link wildfires to ablation of mountain glaciers. To accomplish this objective, the impact of wildfire smoke and LAI deposition on albedo and near-surface meteorology was studied using intensive surface observations, process-based cold regions glacier hydrological modeling, and remote sensing. This study was conducted at the well-instrumented Athabasca Glacier Research Basin, which is part of the Columbia Icefield in the Canadian Rockies, for the 2015–2020 melt seasons.

2. Methods

2.1. Study Site and Data: Athabasca Glacier Research Basin

The Canadian Rockies are the headwaters of some of the largest rivers in North America and provide an important part of the streamflow in late summer for the downstream environments, especially during dry, warm summers (Bash & Marshall, 2014; Comeau et al., 2009; Jost et al., 2012; Naz et al., 2014). Within the Canadian Rockies, the Columbia Icefield is the hydrological apex of North America, contributing runoff that ultimately reaches the Arctic, Atlantic and Pacific oceans through the Mackenzie, Saskatchewan and Columbia rivers (Figure 1).

Smoke from wildfires occurring in heavily forested British Columbia, just west of the Columbia Icefield, tends to travel eastward along prevailing westerly flows to the Canadian Rockies. In the last five years, fire activity upwind of the Columbia Icefield has been highly variable and includes the two worst fire seasons ever recorded, 2017 and 2018. In 2018 alone, over 1.35 million hectares burned, over 2200 properties were evacuated, and the cost of wildfire suppression reached $615 million (Government of B.C., 2019). Below average fire activity occurred in 2016, 2019 and 2020.

Over the same period (2015–2020), two automated weather stations (AWS) operated in Athabasca Glacier Research Basin, which comprises an outlet glacier of the Columbia Icefield and its proglacial landscape: AWS_{ice}, on the glacier toe at 2177 m a.s.l., and $AWS_{moraine}$, less than 1 km from the glacier terminus, at elevation 1966 m a.s.l. (Figure 1, Table S1 in Supporting Information S1). The stations observed air temperature (T_a) and relative humidity (RH) using Rotronic temperature and humidity probe, wind speed (U) using RM Young Wind Monitors, incoming and outgoing short (SW) and longwave (LW) radiation using Kipp and Zonen CNR4 net radiometers, and snow depth and ice elevation using Campbell Scientific Canada SR50 ultrasonic depth rangers. Precipitation was observed at $AWS_{moraine}$, using a Meteorological Services tipping bucket rain gauge and an Alter-shielded Geonor weighing precipitation gauge. The precipitation gauge suffered from an instrument malfunction during the 2019 melt season and was infilled with three other stations in the vicinity using an inverse distance weighting interpolation method. A Wingscapes, 8.0-megapixel, time-lapse camera was mounted on the $AWS_{moraine}$ pointed towards the Athabasca Glacier and provided visibility, smoke, precipitation type and cloud observations. The time-lapse camera recorded pictures at 8:00, 13:00 and 16:00 local time.

The seasonal period analyzed here, July 1st to September 15th, referred to as the melt season, includes the co-occurrence of the primary glacier melt period and the regional wildfire season. The range of years from 2015 to 2020 includes both high and low wildfire occurrence and cool, wet and warm, dry years.

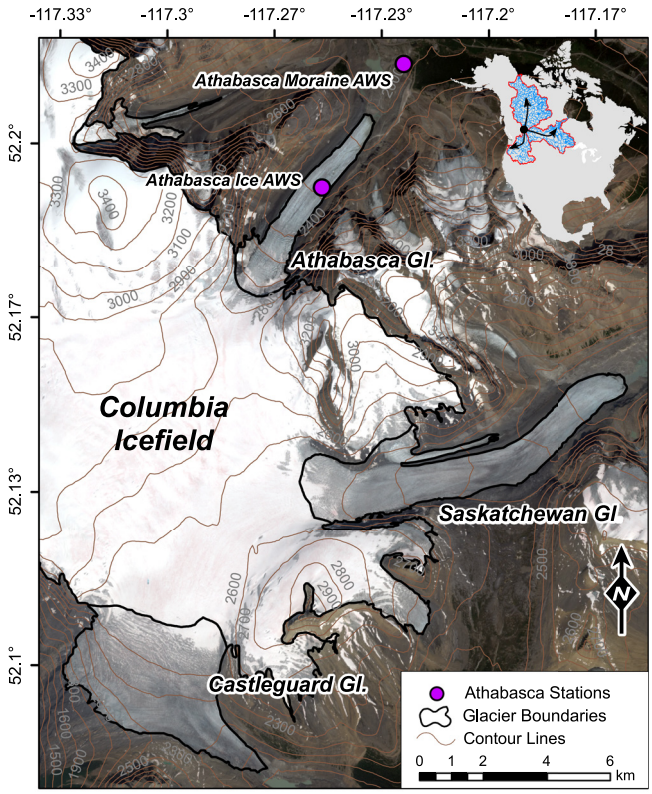

Figure 1. Map of the Columbia Icefield with the three main outlet glaciers: Athabasca Glacier, Saskatchewan Glacier and Castleguard Glacier, with the location of the automated weather station showed with purple circle. The Columbia Icefield is the headwater of drainage basin reaching the Atlantic, Pacific and Arctic Oceans, as shown by the inset map of North America. The background imagery is from 8 August 2018 obtained from Sentinel-2 and the elevation line are derived from Shuttle Radar Topography Mission digital elevation model obtained in February 2000.

2.2. Defining the Characteristic Meteorological Conditions

Time-lapse images were taken three times a day at the $AWS_{moraine}$ station for the 2015–2020 melt season. These were classified manually according to the weather type: predominantly clear sky, a mix of sun and cloud, predominantly cloudy, light smoke or dense smoke (Figure 2). Light and dense smoke were selected based on the attenuation of distant visual features in the visual images, such as snow patches, rock outcrops and clouds. In light smoke conditions, these features were still visible, but in dense smoke conditions, it was difficult to discern the clouds and the distant mountain landscape. The resulting time series of Athabasca weather was used to select representative days for each weather type, defined as when two consecutive images out of three show the same weather type. The measured air temperature, relative humidity and incoming shortwave and longwave radiation for these representative days were extracted from the AWS_{ice} record and compiled to obtain average daily meteorological conditions for each of the weather types. These representative meteorological conditions are used to investigate how the presence of smoke affects the atmospheric conditions at the Athabasca glacier.

2.3. Modeling Approach: Isolating the Impact of Smoke and LAI

The impact on the surface melt of both the changes in ice albedo and on short and longwave irradiance was diagnosed using a new point-based surface energy balance model developed in the Cold Region Hydrological Modeling platform (CRHM, Pomeroy et al., 2007, 2016) using an hourly energy budget approach (Equation 1):

$$M = SW_{in}(1 - \alpha) + LW_{net} + Q + H + P \quad (1)$$

where M is the energy available for melt, SW_{in} in the shortwave irradiance, α is the surface albedo, longwave (LW_{net}) is net longwave radiation, Q is the turbulent latent heat flux, H is the turbulent sensible heat flux and P is the energy advected from precipitation. The turbulent fluxes were calculated using a katabatic wind parametrization from Oerlemans and Grisogono (2002). Model forcings of air temperature, relative humidity, wind speed, albedo, and shortwave and longwave irradiance were observed at the AWS_{ice}, and precipitation at the $AWS_{moraine}$. The model was evaluated using measured surface ablation at AWS_{ice} which was available intermittently during the 2016–2020 melt seasons.

The model was run for the 2015–2020 melt seasons (July 1st–September 15th) following four scenarios to isolate the impact of attenuated irradiance due to smoke and decreased albedo due to LAIs. LAIs are defined as all surface particulates and impurities that contribute to the decrease in surface albedo, including dust, black carbon and microbial growth (Skiles et al., 2018). The four scenarios are shortly described below and in Figure 3:

1. No Fire: Removes the impact of fire activity for both the glacier surface and the atmosphere, by using a standard mountain glacier ice albedo of 0.3 and modeled smoke-free irradiance.
2. With Smoke: Isolates the impact of the radiation attenuation due to smoke by using the measured irradiance with the standard ice albedo of 0.3.
3. With LAIs: Isolates the impact of the albedo reduction by LAIs by using measured albedo with modeled smoke-free irradiance.
4. With Fire: Corresponds to observed conditions and combines the measured albedo reduction and the measured irradiance attenuation to simulate fire activity.

Measured albedo was calculated as the ratio of shortwave reflection to irradiance measured from the AWS_{ice}. The no-LAI surface albedo in scenario (1) and (2) was set to a reference value for clean glacier ice, 0.3 (Benn & Evans, 2010). On days when smoke was detected in the time-lapse imagery, the shortwave and longwave

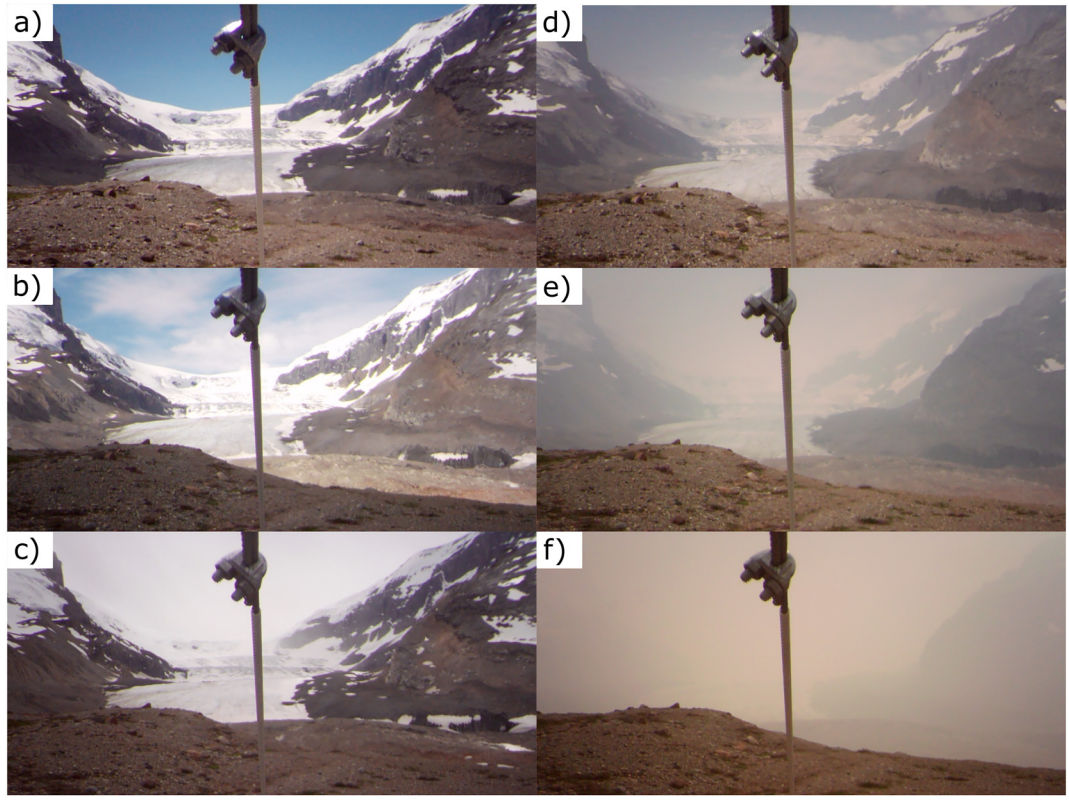

Figure 2. Example of time-lapse images for (a) clear, (b) mix of sun and cloud, (c) cloudy, (d) light smoke, and (e and f) dense smoke, extracted from the 2017 melt season.

irradiance were corrected separately to remove the effects of smoke in scenario (1) and (3). On days when no smoke was detected, measured irradiance was used. Both irradiance corrections used a transmissivity correction. The temperature, relative humidity and wind speed were not adjusted amongst the four scenarios.

The presence of smoke in the atmosphere absorbs shortwave radiation, reducing the irradiance at the surface by decreasing the transmittance (McKendry et al., 2019; Stone et al., 2008). Therefore, transmissivity on smoky days is lower than on clear days. To simulate smoke-free shortwave irradiance, $SW_{in\ mod}$, the transmissivity of smoky days needs to be increased to a value corresponding to smoke-free days. To achieve this, the clear-sky transmissivity was calculated as the average transmissivity occurring during days classified as clear in the time-lapse imagery classification. Then, the difference in transmissivity between measured smoky days and the average clear-sky transmissivity Δ_τ was calculated (Equation 2). This difference in transmissivity was used to calculate

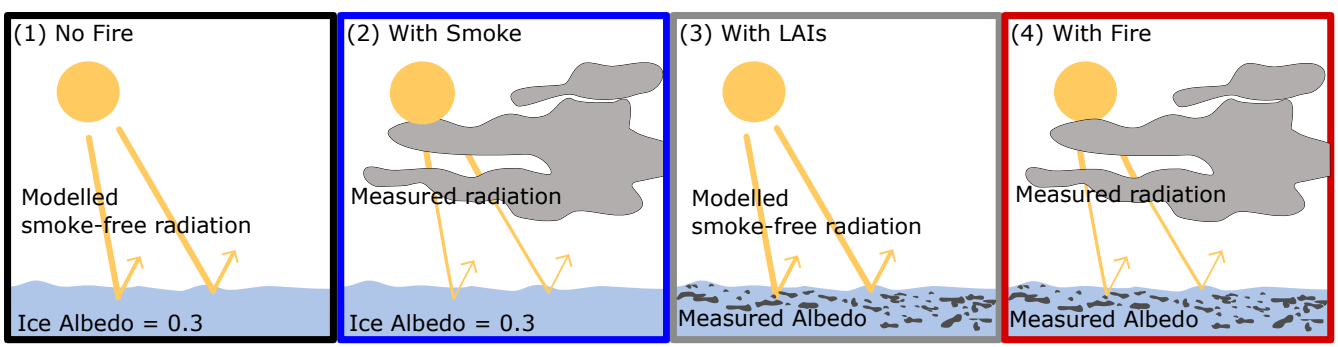

Figure 3. Conceptual representation of the four modeling scenarios. The framing color corresponds to the line color in Figure 8.

the missing shortwave irradiance Δ_{SWin}, linked to the presence of smoke (Equation 3). The missing irradiance was calculated for each smoky day and added to the measured shortwave irradiance to estimate the simulated smoke-free irradiance $SW_{in\,mod}$ (Equation 4).

$$\Delta_{\tau} = \tau_{\text{meas smoky}} - \underline{\tau_{\text{clear}}} \tag{2}$$

$$\Delta_{SW_{in}} = SW_{meas} * \Delta_{\tau} \tag{3}$$

$$SW_{in\,mod} = SW_{in\,meas} + \Delta_{SW_{in}} \tag{4}$$

where $SW_{in\,meas}$ is the shortwave irradiance (Wm^{-2}) measured at the AWS_{ice}, τ_{clear} and $\tau_{meas\,smoky}$ are the average measured clear sky transmissivity and the measured smoky transmissivity, calculated as the ratio of measured shortwave irradiance to the theoretical extraterrestrial incoming shortwave radiation flux—both to horizontal planar surfaces.

To remove the influence of smoke on the longwave irradiance, a factor, f_{lw}, was calculated based on the difference between simulated longwave irradiance with smoky transmissivity and with the average clear-day transmissivity τ_{clear} (Equation 5). The theoretical simulated longwave irradiance was calculated following Sicart et al. (2006, Equation 6). The measured longwave factor was then used to adjust the measured longwave irradiance to remove the impact of the smoke (Equation 7).

$$f_{lw} = \frac{LW_{theo\,clear}}{LW_{theo\,smoky}} \tag{5}$$

$$LW_{theo} = 1.24 * \left(\frac{e_a}{T}\right)^{\frac{1}{7}} * (1 + 0.44 * RH - 0.18 * \tau) * \sigma T^4 \tag{6}$$

$$LW_{in\,mod} = LW_{in\,meas} * f_{lw} \tag{7}$$

where e_a is the water vapor pressure (kPa), RH is the relative humidity (%), σ is the Stefan Boltzmann constant (5.67×10^{-8} Wm^{-2} K^{-4}) and T is the air temperature (K) and τ_{meas} is measured transmissivity.

This transmissivity-based approach to simulate smoke-free conditions preserves the daily signature of the measured irradiance. For example, a day with smoke detected in the time-lapse imagery, but also with the low shortwave irradiance associated with cloudy weather, will still have low shortwave irradiance after the impact of the smoke is removed.

2.4. Spatial Albedo Estimates

To upscale the results of the point albedo measured at the AWS_{ice}, the change in albedo over the three largest outlet glaciers of the Columbia Icefield was analyzed using remote sensing imagery over the 2016–2020 melt seasons (Bertoncini et al., in review) For 12 Sentinel-2 images, high-resolution albedo over the glaciers was estimated using Moderate Resolution Imaging Spectroradiometer (MODIS) data to model the bidirectional reflectance of snow and ice, following the approach detailed in Bertoncini et al. (in review). The spatial variations in albedo across each glacier toe were assessed for each melt season, but also amongst melt seasons.

3. Results and Discussion

3.1. Seasonal Weather Types and Meteorological Conditions

The time-lapse image classification reveals that, for the 2015–2020 melt seasons, the weather at Athabasca glacier was predominantly cloudy, with 50% of images analyzed categorized as cloudy, in contrast to 15% for clear skies, 24% for a mix of sun and clouds, and 5% and 6% for light and dense smoke (Figure 4). The presence of smoke differs from year to year. The 2016 and 2019 melt seasons show no presence of smoke. In 2015, smoke was detected in only 7% of the images, concentrated in late August, and in 2020, only 4% of images show smoke, concentrated close to September 15th on late September. The 2017 and 2018 melt seasons have the

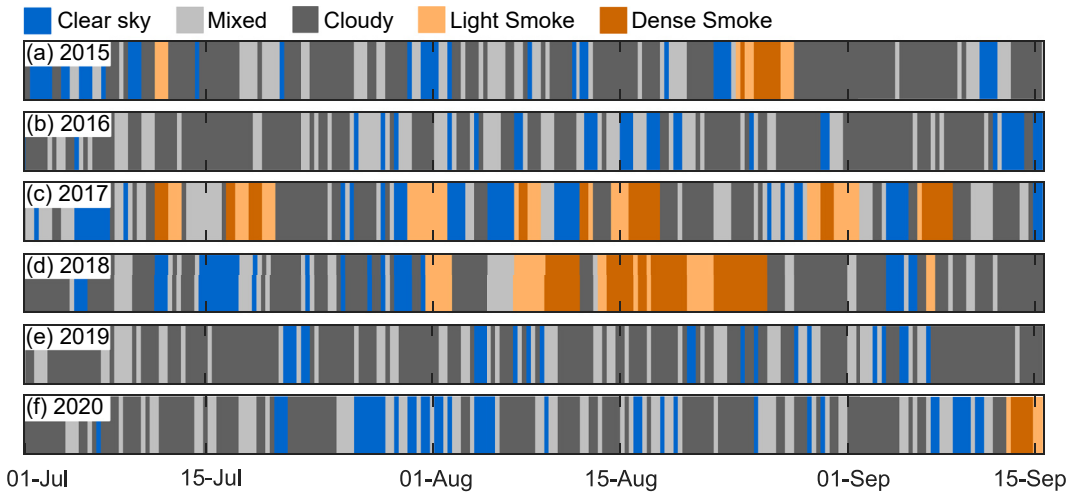

Figure 4. Weather type at Athabasca glacier obtained from the time-lapse image classification for the 2015 to 2020 melt seasons.

largest presence of smoke, with 29% and 26% of images showing either light or dense smoke, but with different timing. Detailed numbers of images for each weather type per year can be found in Table S2 of Supporting Information S1.

Meteorological conditions on the glacier in the five melt seasons were not associated with smoke activity, assessed as the number of days with dense or light smoke in a given year (Table 1). Mean air temperature over each melt season varied by 1.85°C between the warmest (2017) and the coldest (2016) years. The years with smoke were not consistently warmer than years without smoke. Similarly, even though smoke years (2015, 2017, 2018) were drier than no-smoke years (2016, 2019), the annual smoke activity did not correlate with the humidity of the given year. Precipitation similarly was lower for the intense fire season of 2017 and 2018, but also for 2020 with few fires. The only consistent pattern is for the measured ice surface albedo, which decreased from a summer average of 0.29 in 2015 to 0.20 in 2018, after which it remained low (Figure 5). However, the low albedo values in 2020 increased moderately in late August compared to the seasonan progression of albedo in 2018 and 2019, suggesting a partial recovery that may be associated with some surface LAIs being washed away by meltwater. These low ice albedos are similar to what have been measured on other glaciers in the Canadian Rockies during similar forest fire activity, such as on Haig Glacier, where albedo as low as 0.12 were recorded in 2003 and 2017, after summers of high forest fire activity (Ebrahimi & Marshall, 2015; Marshall & Miller, 2020). The link between decreasing surface albedo and wildfire activity in the region was also discussed by Williamson and

Table 1
Seasonal Mean Meteorological Conditions From July 1 to September 15, Except for Albedo Which Was Calculated for July 15–August 15, as There Were No Fresh Snowfall Event That Would Influence the Calculation of the Ice Albedo for That Period

	2015	2016	2017	2018	2019	2020
Air Temperature (°C)	6.7	5.9	7.7	6.5	6.6	6.9
Relative Humidity (%)	65	72	61	66	70	64
Shortwave Irradiance (Wm^{-2})	202	192	207	208	206	221
Longwave Irradiance (Wm^{-2})	301	305	297	300	304	302
Wind Speed (ms^{-1})	5.3	4.6	5.6	5.3	5.4	6.4
Total precipitation (mm)	147	144	91	139	126	116
Albedo (minimum)	0.29 (0.24)	0.24 (0.23)	0.26 (0.21)	0.20 (0.16)	0.20 (0.17)	0.20 (0.17)

Note. The glacier surface was snow-free at AWS_{ice} every year in this period. All variables were from AWS_{ice} except precipitation, which was measured at $AWS_{moraine}$.

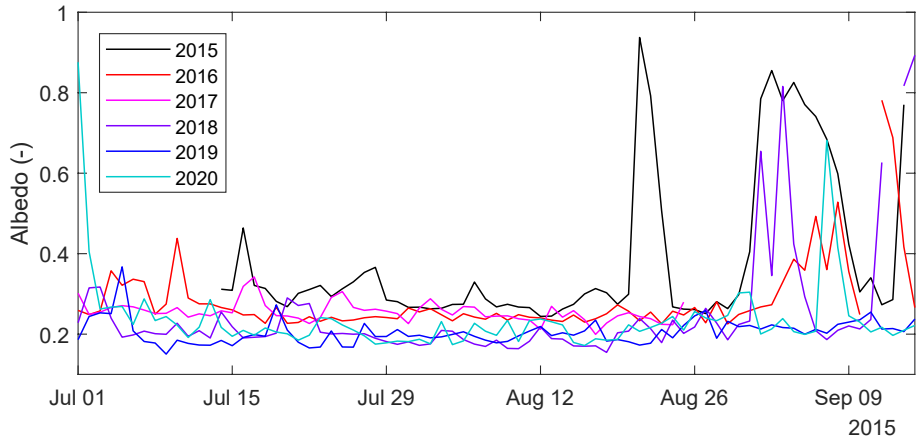

Figure 5. Daily measured Athabasca Glacier albedo for the 2015–2020 melt seasons.

Menounos (2021), who found a strong correlation between glacier albedo decrease over the 2000–2019 period and aerosol optical depth, a proxy for wildfire-generated smoke.

3.2. Average Meteorological Conditions Per Weather Type

Meteorological conditions on smoky days contrasted with those on non-smoky days (Figure 6). Meteorological conditions were on average warmer on smoky days than cloudy or mixed weather days, with average daily temperatures of 8.0°C for light smoke and 8.6°C for dense smoke, compared to 7.6, 7.0 and 5.4°C for clear, mixed and cloudy weather (Figure 6a). Smoky days also underwent a subdued diurnal variation compared to clear days; a variation that was similar to those observed during cloudy weather. This is also visible in the relative humidity (Figure 6b), where smoky days were drier than other weather types, and once again with lower diurnal fluctuation.

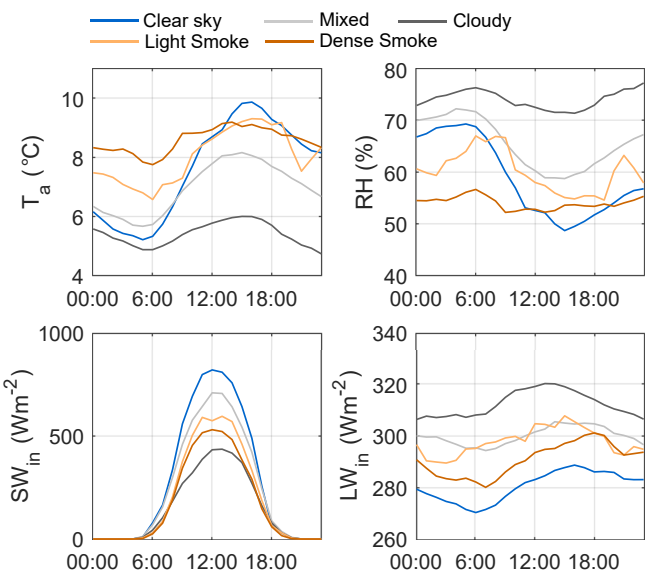

Figure 6. Average daily meteorological conditions observed on Athabasca Glacier for the different weather types (clear sky, mixed of sun and clouds, cloudy, light smoke and dense smoke); (a) shortwave irradiance, (b) longwave irradiance, (c) air temperature, (d) relative humidity.

A clear difference amongst weather types is apparent for the characteristic shortwave irradiance (Figure 6c). As expected, the highest shortwave irradiance occurred on clear days, with mean daily peaks of 820 W m^{-2} and SW_{in} on cloudy days was significantly reduced, with the mean daily peak SW_{in} reduced to 433 W m^{-2}. Irradiance on light and dense smoke days was between that on clear and cloudy days, with mean daily peak shortwave irradiance reduced by 225 W m^{-2} for light smoke and 290 W m^{-2} for dense smoke compared to irradiance on clear days.

Longwave irradiance on both light and dense smoke days was between that on clear and cloudy days, with a daily average irradiance of 298 W m^{-2} and 291 W m^{-2}, respectively. Longwave irradiance was higher for cloudy days, averaging 312 W m^{-2}, compared to clear days, on which it averaged 281 W m^{-2} (Figure 6d). The average meteorological conditions for each weather type per melt season are presented in Figure S3 of Supporting Information S1.

3.3. Adjusted Irradiance Based on Transmissivity

The transmissivity-based adjustment to the observed irradiance to simulate the removal of the smoke has contrasting effects on the shortwave and longwave irradiance that result in a very small impact on net radiation (Figure 7). The transmissivity-based adjustment to the observed irradiance to simulate the removal of the smoke has contrasting effects on the shortwave and

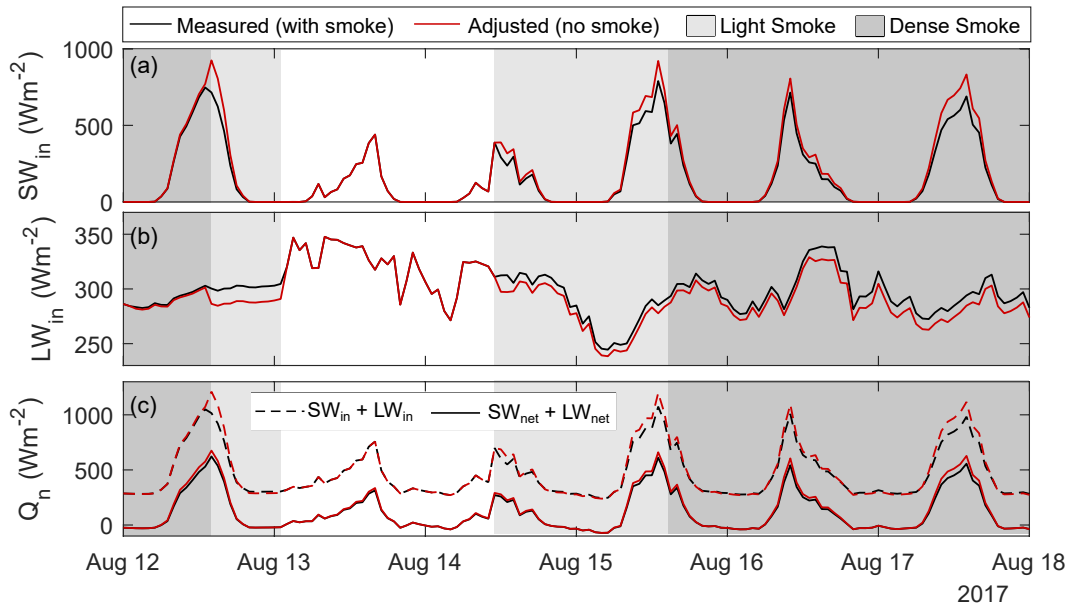

Figure 7. Measured (with smoke) and adjusted (no smoke) shortwave (SW)(a) and longwave (LW) (b) irradiance, with all-wave irradiance ($SW_{in} + LW_{in}$, dashed) and net radiation ($SW_{net} + LW_{net}$, full) in c for a selected smoky period in the 2017 melt season.

longwave irradiance that result in a very small impact on net radiation (Figure 7). The smoke-removal adjustment increased shortwave irradiance by, on average, 14 and 21 W m^{-2} for the light and dense smoke conditions respectively, with respective hourly maxima increasing by 193 and 209 W m^{-2} occurring during times of peak irradiance. In contrast, the corresponding smoke-removal adjustment decreased longwave irradiance by, on average, 3.6 and 7.2 W m^{-2} for light and dense smoke respectively, with hourly maxima decreasing by 16 and 23 W m^{-2} respectively. The large decrease in shortwave irradiance due to attenuated transmittance during smoky conditions is partly mitigated by increased longwave irradiance. These irradiance changes result in an average increase in all-wave irradiance of 10 and 13 W m^{-2} when adjusting for light and dense smoke, with hourly maxima increasing by 179 and 195 W m^{-2}, respectively. These adjustments to shortwave and longwave irradiance are consistent with the observed differences in irradiance between clear and smoky conditions (Figures 6c and 6d), as the presence of smoke reduces shortwave but increases longwave irradiance.

However it is the absorption of the shortwave and longwave irradiance at the ice surface to form net radiation that determines the impact of smoke on glacier melt. Approximately 99% of longwave irradiance was absorbed by the ice surface assuming an emissivity of 0.99, but only 77% of the shortwave irradiance was absorbed given the average measured ice albedo of 0.22 and 0.24 during light and dense smoke conditions. This difference in absorption reduced the effect of the transmittance attenuation on shortwave irradiance. When considering the changes in shortwave and longwave irradiance and absorption, and using the measured albedo values, the presence of smoke reduces the net radiation at the ice surface by 15 W m^{-2} for both light and dense smoke, with hourly maximal reductions of 107 and 114 W m^{-2}, respectively compared with adjusted, smoke-free conditions. This 15 W m^{-2} average reduction in net radiation due to the presence of smoke results in a reduction in ice melt of less than 4 mm day^{-1} compared to smoke-free conditions. Further examples of the adjusted incoming shortwave and longwave irradiance are available in Figures S1 and S2 of Supporting Information S1.

3.4. Melt Model Evaluation

Cumulative melt was measured for most of the 2016–2020 melt seasons, with gaps when station maintenance was performed. The CRHM surface melt model predicted observations of surface melt well, with a mean relative error of 3% for all observation periods, ranging between an overestimation of 9% to an underestimation of 4% for individual melt seasons. This corresponds to errors ranging between 6 mm day^{-1} in 2020 to less than 1 mm day^{-1}

Table 2
Point Melt Model Evaluation

Period (number of days)	Observed melt (m)	Modeled melt (m)	Error (m)	Error (%)
July 14–31 August 2016 ($n = 48$)	2.79	2.63	0.15	6
Jul 20–6 August 2017 ($n = 17$)	0.9	0.94	−0.04	−4
Jul 1st–12 September 2018 ($n = 73$)	3.83	3.86	−0.03	−1
Jul 1st–15 September 2019 ($n = 77$)	4.24	4.16	0.09	2
Jul 14–6 September 2020 ($n = 54$)	3.5	3.19	0.32	9
All periods ($n = 323$)	17.81	17.25	0.56	3

Note. The number of days used in the model evaluation is indicated in parenthesis in the period column.

in 2018. The cumulative melt observed at the AWS_{ice} and melt compiled by the model are presented in Table 2 and Figure S4 of Supporting Information S1.

3.5. Isolating the Effect of Smoke and LAI

To illustrate the impact of forest fire activity on the daily melt volume, hourly melt from the four scenarios for days with variable weather conditions is shown in Figures 8a and 8b and Table S3 of Supporting Information S1. These 12 days are representative of the patterns seen throughout the 2015–2020 melt seasons, including smoky days with clouds, smoky days with clear skies (without clouds), and days without smoke. On smoky-cloudy days such as 14 August 2018, the radiation attenuation ("With Smoke" scenario) and the darker albedo ("With LAIs" scenario) have opposing impacts of similar magnitude on ice melt. For example, on 14 August 2017, the presence of smoke reduced melt by 4 mm, but the darker surface albedo increased melt by 4 mm, resulting in the "No Fire" and the "With Fire" scenario showing the same daily melt. Similarly, the following day, the presence of smoke reduced melt by 2 mm, but the darker albedo increased melt by 3 mm. On smoky-clear days, the impact of the presence of LAI typically outweighed the impact of the presence of smoke. For example, on 15 August 2018, the presence of smoke reduced melt by 4 mm, but the presence of LAI increased melt by 9 mm. On the following day, smoke reduced melt by 1 mm, and the LAI increased melt by 8 mm. Therefore, it is important to consider the weather associated with the smoke (smoky and clear or smoky and cloudy), to assess the compensating impacts of reduced atmospheric transmissivity by smoke, affecting both short and longwave irradiance, and albedo reduction by LAIs.

Noting that smoky conditions only occurred during 11% of the 2015–2010 melt seasons, the four simulations show that, at the seasonal time scale, the large increase in melt due to albedo reduction overcomes the small reduction in melt due to reduced atmospheric transmissivity (Figures 8c–8h, Table S4 in Supporting Information S1). The compensatory effects of reduced atmospheric transmissivity, which reduces melt, and albedo reduction, which increases melt, are particularly visible in 2017 and 2018. Both these years had smoke detected and low albedo observed on Athabasca Glacier. In 2017, reduced atmospheric transmissivity decreased melt by 1.4% compared to the "No Fire" scenario, but the presence of LAI increased melt by 4.9%, resulting in a total increase in melt of 3.3%. This is equivalent to an increase in melt of 0.12 m w.e. per year. In 2018, the year with the greatest upwind fire activity in historical record, radiation attenuation reduced melt energy by 0.9%, but albedo reduction increased melt by 11.1%, for a net increase in melt of 10.2%, or 0.35 m w.e. per year, compared to the no-fire simulation.

The following year, 2019, no smoke was detected at Athabasca, but the simulations indicate that, with albedo remaining as low as 0.17, the albedo reduction caused an increase in melt of 11.5% (0.42 m w.e. per year.). In 2020, smoke was detected only in the last few days of the melt season, and the reduced albedo simulation shows an increase in melt of 9.6% compared with the no-fire simulation (0.37 m w.e. per year). These 2 years are very similar and much higher than the 4.5% increase in melt due to albedo reduction reported in Magalhães et al. (2019) for the tropical Andes.

This low observed albedo of 0.17, remaining low after two summers of intense fire activity, also indicates that the albedo reduction continues even after fire activity ceases. Even without deposition of new smoke-derived LAIs,

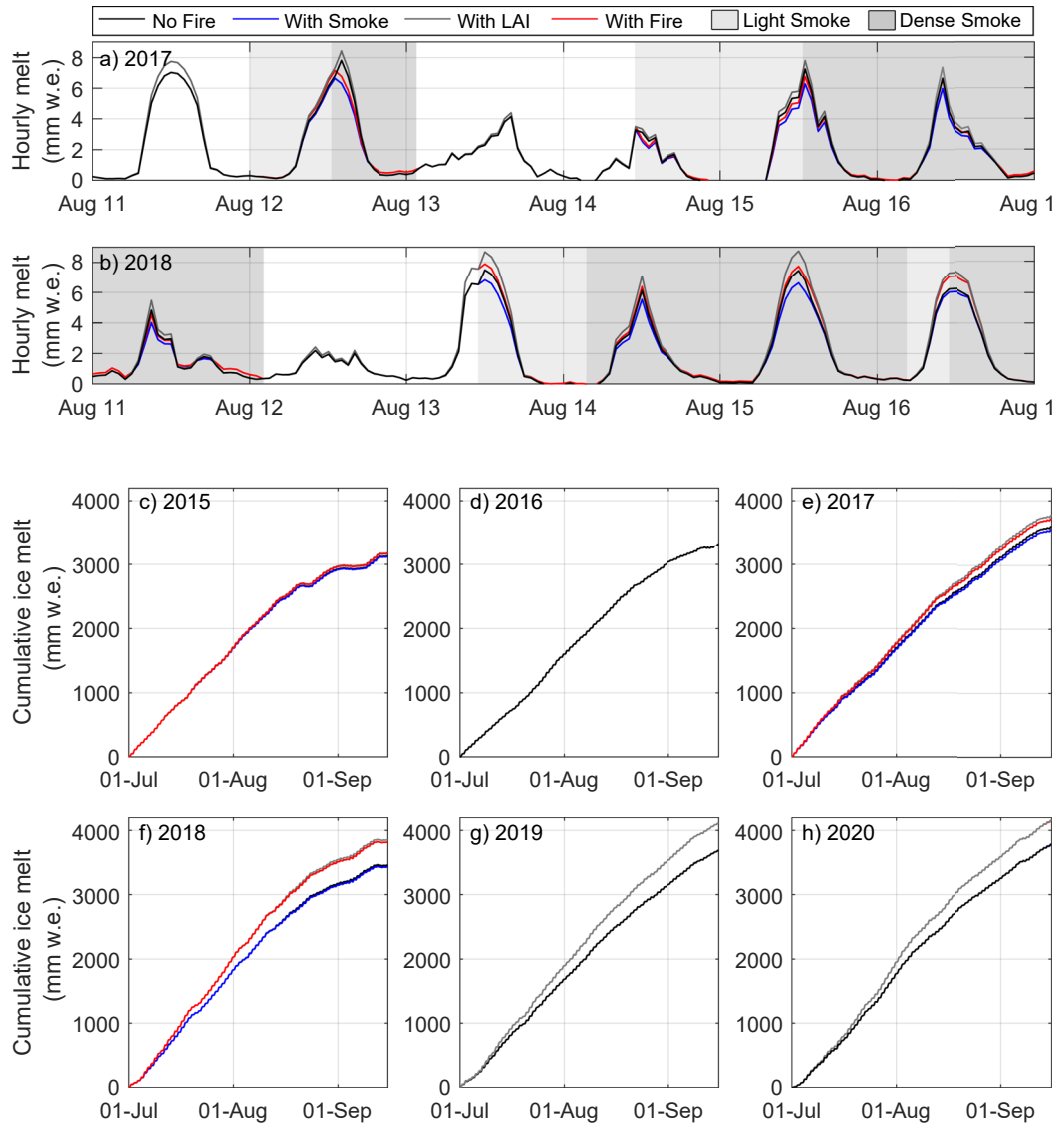

Figure 8. Simulated hourly melt for the four scenarios (No Fire, With smoke, With light-absorbing impurities (LAIs), With Fire) in (a) 2017, and (b) 2018, and simulated cumulative seasonal melt for each of the 2015–2020 seasons in (c–h) for the four smoke and LAI scenarios. The days and seasons with only the "No fire" (black) and "No LAIs" (gray) lines correspond to days or seasons with no smoke detected at the Athabasca Glacier.

and likely some removal of LAIs from the surface meltwater, the albedo remains low. This may be linked with microbial growth on the glacier ice, as carbon deposition on snow and ice surfaces can feed microbial and algal growth, which then causes a further reduction in albedo (Cook et al., 2017; Jones et al., 2001; Stibal et al., 2012; Tedstone et al., 2019).

These melt simulations assess how wildfire smoke, through changes to both irradiance and albedo, can influence surface melt. The difference in temperature and humidity between smoky and non-smoky conditions, though observed on site, were not assessed in these melt simulations even though they could influence melt rates. Warmer and less humid conditions can be both a cause and a consequence of wildfire activity, and so untangling the causality between wildfire activity, temperature and humidity in this modeling experiment was considered out of the scope of this study.

Worldwide, glaciers have witnessed an accelerating mass loss since 2000 (Hugonnet et al., 2021), and ongoing glacier retreat is well-documented for the Canadian Rockies (DeBeer & Sharp, 2007; DeBeer et al., 2016;

Tennant et al., 2012; Tennant & Menounos, 2013). Glacier loss across western North America shows a heterogeneous regional pattern since 1985, with the mass loss rate slowing in the 2000–2009 period and accelerating for the 2009–2018 period, with the regional and temporal variability possibly linked with a shift in regional meteorological conditions from upper level zonal winds (Menounos et al., 2019). Glaciers in Western Canada, and specifically in the Canadian Rockies, are expected to be largely ablated by the end of the century (Clarke et al., 2015; Huss & Hock, 2018). The increase is surface melt from lowered surface albedo driven by wildfire activity presented in this study provides further insights on the complex mechanism and feedback linking glacier mass balance and climate forcings.

3.6. Spatially Distributed Albedo Change From Remote Sensing

The three outlet glaciers show a range of albedos (Figure 9), which demonstrates the importance of complementing point-based analysis with areal estimates. For the Athabasca Glacier, satellite-derived albedo was obtained both for the entire glacier area and for the pixel corresponding to the location of the AWS_{ice}, with a spatial resolution of 20 × 20 m. Glacier-wide albedos for the Athabasca Glacier were higher than at the AWS_{ice} (Figure 9a). This difference is likely linked to late summer snow patches lingering at the higher elevation of the glacier area (Figures 9b–9d). These patches were particularly visible in the 2020 melt season, following a wet and cool spring which caused snowcover to persist into late summer on the Columbia Icefield. The partial recovery in measured surface albedo for the 2020 late melt season is evident in the glacier-wide albedo and for the pixel corresponding to the location of the AWS_{ice}, with the remotely-sensed albedos increasing from 0.293 to 0.327, and 0.186 to 0.233 respectively over the melt season, which suggests the possibility of LAIs being removed from the surface.

The glacier-wide albedo of both the Castleguard and Saskatchewan Glacier show similar trends, with low albedo in 2019 despite the lack of forest fire activity during that melt season, and recovery during the 2020 melt season, with the albedos rising to the more typical clean-ice albedo of 0.3.

The Castleguard and Saskatchewan glaciers showed the largest variability in albedo. For the Castleguard, this is linked to a lingering high-albedo snow patch below the glacier outline, and some dark or debris covered ice with a very low albedo observed near its toe (Figures 9b–9d). For the Saskatchewan, the variable snowline and a dark ice zone adjacent to low-lying bare soil and rock near the middle of the glacier results in larger spatial variability than the Athabasca.

4. Conclusions

The impacts of upwind forest fire activity on glacier melt were investigated through analysis of field observations, modeling experiments and remote sensing imagery for the 2015–2020 melt seasons at Athabasca Glacier and the surrounding Columbia Icefield in the Canadian Rockies of western Canada. At the Athabasca Glacier, upwind forest fire activity influenced surface glacier melt in two ways; firstly, through decreasing the glacier albedo from soot deposition following smoke drifting over the glacier and secondly, through the direct impact of the atmospheric conditions above the glacier on reducing shortwave irradiance, increasing longwave irradiance and reducing net radiation. Days with smoke were warmer and drier, had lower shortwave irradiance and greater longwave irradiance compared to non-smoky, clear days. However, the compensatory impacts of lower shortwave and higher longwave irradiance dampened the reduction in net radiation for smoky days.

The compensatory effects of soot deposits and subsequent microbial growth, which reduced albedo, and smoke in the atmosphere above the glacier, which reduced atmospheric transmissivity, were analyzed using a point-based energy balance model. Even though smoke slightly increased longwave irradiance, the attenuation of the shortwave irradiance is greater, resulting in an overall reduction in all-wave irradiance and a reduction in net radiation of 15 W m^{-2} during smoky conditions, compared to non-smoky conditions. For years when wildfire smoke was detected, reduced all-wave irradiance partly compensated for the effects of reduced albedo on melt energetics, giving a net increase in melt of only 6.75%. However, in years without smoke, the low albedo from antecedent soot deposits increased seasonal ice melt by more than 10%, or 0.42 m w.e. per year. In 2019, the suppressed albedo resulted in an increased melt of 0.42 m. w.e. per year, or 10.2% of the simulated melt for the July 15–September 15 period compared to when simulated with a standard ice albedo of 0.3. Similarly, in 2020, the simulated melt increased by 0.37 m. w.e. per year, or 8.9% of the simulated melt.

10.1029/2022EF002685

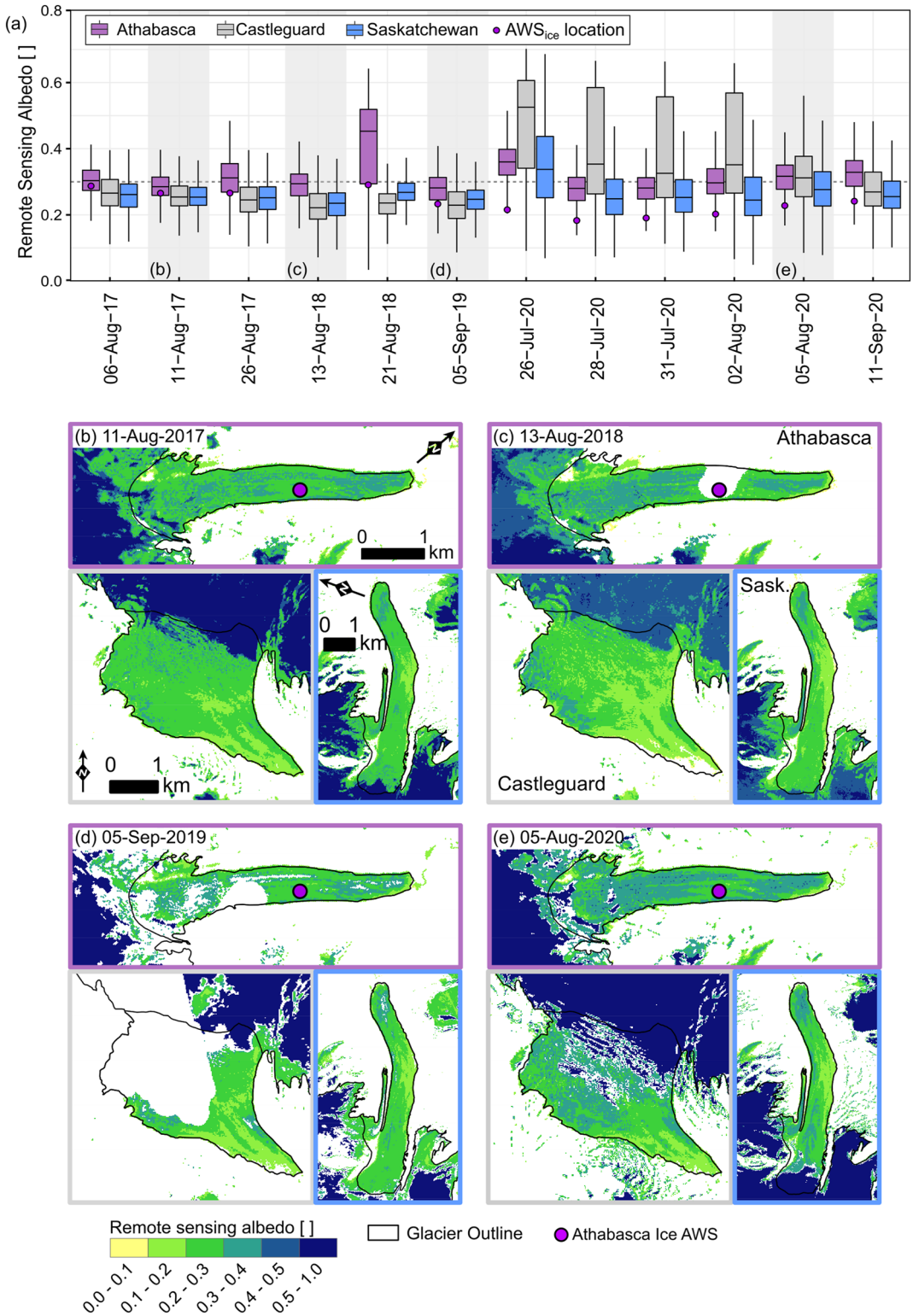

Figure 9. Remote sensing albedo for the Athabasca, Castleguard and Saskatchewan Glaciers for 12 dates in the 2017–2020 melt seasons (a), with spatial end-of-summer albedo (dates with the lowest glacier albedo for each season, highlighted in gray) shown in b-e. Please note the change in color gradation for albedo above 0.5. The location of the Athabasca automated weather stations (AWS) is shown as a purple dot in b-d. The horizontal gray line in (a) shows the reference albedo of 0.3 and the purple dot corresponds to the albedo for the pixel where the AWSice is located.

The results from the point-based energy balance model experiment were upscaled by analyzing the areal albedo dynamics using satellite-derived albedos for the three main outlet glaciers of the Columbia Icefield (Athabasca, Saskatchewan and Castleguard glaciers). High-resolution albedo retrievals from 24 Sentinel 2 images, combined with a MODIS snow-kernel used to model the bidirectional reflectance of snow and ice, show that the albedo changes across the three glacier surfaces is consistent with the point-albedo measured on the Athabasca Glacier toe.

This study provides a process-based understanding of the impacts of wildfire activity on the mountain cryosphere. It shows that increased longwave irradiance partly compensates for reduced shortwave irradiance and that reduced net irradiance partly compensates for reduced albedo on smoky days after soot deposition on glaciers. However, the net effect of wildfires in increasing glacier melt is substantial and long lasting due to the reduced albedo. Considering the expected increase in both climate extremes and forest fire activity, coupled with continued decline in mountain glaciers, understanding the processes at play provides a first step toward improved predictions of runoff from these glaciers and less uncertain assessments of the implications of changing glacier hydrology for downstream water resources and sea level rise.

Data Availability Statement

The scripts used to process and analyze the timelapse imagery, meteorological data and energy-balance simulations can be found at: https://github.com/caubrywake/FireAndIce and the meteorological data as well as the time-lapse images analysed can be found at: https://www.hydroshare.org/resource/5ef34291cdcd44a4ac2dcdddbaa0e310/.

Acknowledgments
The authors wish to acknowledge funding from the Natural Sciences and Engineering Research Council of Canada in the Discovery Grants and Vanier and Michael Smith Scholarship programs, Alberta Innovation, the Canada Research Chairs programme and the Canada First Excellence Research Fund's Global Water Futures programme.

References

Abatzoglou, J. T., Williams, A. P., & Barbero, R. (2019). Global emergence of anthropogenic climate change in fire weather indices. *Geophysical Research Letters*, *46*(1), 326–336. https://doi.org/10.1029/2018GL080959

Bash, E. A., & Marshall, S. J. (2014). Estimation of glacial melt contributions to the Bow River, Alberta, Canada, using a radiation–temperature melt model. *Annals of Glaciology*, *55*(66), 138–152. https://doi.org/10.3189/2014AoG66A226

Bedia, J., Herrera, S., Camia, A., Moreno, J. M., & Gutiérrez, J. M. (2014). Forest fire danger projections in the Mediterranean using ENSEMBLES regional climate change scenarios. *Climatic Change*, *122*(1–2), 185–199. https://doi.org/10.1007/s10584-013-1005-z

Benn, D., & Evans, D. J. A. (2010). *Glaciers and glaciation*. Hodder Education.

Burles, K., & Boon, S. (2011). Snowmelt energy balance in a burned forest plot, Crowsnest Pass, Alberta, Canada. *Hydrological Processes*, *25*(19), 3012–3029. https://doi.org/10.1002/hyp.8067

Clarke, G., Jarosch, A. H., Anslow, F. S., Radic, V., & Menounos, B. (2015). Projected deglaciation of western Canada in the twenty-first century. *Nature Geoscience*, *8*(5), 372–377. https://doi.org/10.1038/ngeo2407

Comeau, L., Pietroniro, A. A., & Demuth, M. N. (2009). Glacier contribution to the North and South Saskatchewan Rivers. In *Hydrological processes* (Vol. 23, pp. 2640–2653). https://doi.org/10.1002/hyp.7409

Conway, H., Gades, A., & Raymond, C. F. (1996). Albedo of dirty snow during conditions of melt. *Water Resources Research*, *32*(6), 1713–1718. https://doi.org/10.1029/96WR00712

Cook, J. M., Hodson, A. J., Gardner, A., Flanner, M., Tedstone, A. J., Williamson, C., et al. (2017). Quantifying bioalbedo: A new physically based model and discussion of empirical methods for characterising biological influence on ice and snow albedo. *The Cryosphere*, *11*(6), 2611–2632. https://doi.org/10.5194/tc-11-2611-2017

Cook, J. M., Tedstone, A. J., Williamson, C., McCutcheon, J., Hodson, A. J., Dayal, A., et al. (2020). Glacier algae accelerate melt rates on the south-western Greenland Ice Sheet. *The Cryosphere*, *14*(1), 309–330. https://doi.org/10.5194/tc-14-309-2020

DeBeer, C. M., & Sharp, M. (2007). Recent changes in glacier area and volume within the southern Canadian Cordillera. *Annals of Glaciology*, *46*(1), 215–221. https://doi.org/10.3189/172756407782871710

DeBeer, C. M., Wheater, H. S., Carey, S. K., & Chun, K. P. (2016). Recent climatic, cryospheric, and hydrological changes over the interior of western Canada: A review and synthesis. *Hydrology and Earth System Sciences*, *20*, 1573–1598. https://doi.org/10.5194/hess-20-1573-2016

Di Mauro, B., Garzonio, R., Baccolo, G., Franzetti, A., Pittino, F., Leoni, B., et al. (2020). Glacier algae foster ice-albedo feedback in the European Alps. *Scientific Reports*, *10*(1), 1–9. https://doi.org/10.1038/s41598-020-61762-0

Ebrahimi, S., & Marshall, S. J. (2015). Parameterization of incoming longwave radiation at glacier sites in the Canadian rocky mountains. *Journal of Geophysical Research: Atmospheres*, *120*(24), 12536–12556. https://doi.org/10.1002/2015JD023324

Gillett, N. P. (2004). Detecting the effect of climate change on Canadian forest fires. *Geophysical Research Letters*, *31*(18), L18211. https://doi.org/10.1029/2004GL020876

Gleason, K. E., McConnell, J. R., Arienzo, M. M., Chellman, N., & Calvin, W. M. (2019). Four-fold increase in solar forcing on snow in western U.S. burned forests since 1999. *Nature Communications*, *10*(1), 2026. https://doi.org/10.1038/s41467-019-09935-y

Government of B.C (2019). *Wildfire season summary—Province of British Columbia*. Retrieved from https://www2.gov.bc.ca/gov/content/safety/wildfire-status/about-bcws/wildfire-history/wildfire-season-summary

Hock, R. (2005). Glacier melt: A review of processes and their modelling. *Progress in Physical Geography*, *29*(3), 362–391. https://doi.org/10.1191/0309133305pp453ra

Hugonnet, R., McNabb, R., Berthier, E., Menounos, B., Nuth, C., Girod, L., et al. (2021). Accelerated global glacier mass loss in the early twenty-first century. *Nature*, *592*(7856), 726–731. https://doi.org/10.1038/s41586-021-03436-z

Huss, M., & Hock, R. (2018). Global-scale hydrological response to future glacier mass loss. *Nature Climate Change*, *8*, 135–140. https://doi.org/10.1038/s41558-017-0049-x

Immerzeel, W. W., Lutz, A. F., Andrade, M., Bahl, A., Biemans, H., Bolch, T., et al. (2020). Importance and vulnerability of the world's water towers. *Nature*, *577*(7790), 364–369. https://doi.org/10.1038/s41586-019-1822-y

Jones, H. G., Pomeroy, J. W., Walker, D. A., & Hoham, R. W. (2001). *Snow ecology: An interdisciplinary examination of snow-covered ecosystems*. Cambridge University Press.

Jost, G., Moore, R. D., Menounos, B., & Wheate, R. (2012). Quantifying the contribution of glacier runoff to streamflow in the upper Columbia River Basin, Canada. *Hydrology and Earth System Sciences*, *16*(3), 849–860. https://doi.org/10.5194/hess-16-849-2012

Keegan, K. M., Albert, M. R., McConnell, J. R., & Baker, I. (2014). Climate change and forest fires synergistically drive widespread melt events of the Greenland Ice Sheet. *Proceedings of the National Academy of Sciences of the United States of America*, *111*(22), 7964–7967. https://doi.org/10.1073/pnas.1405397111

Kilpeläinen, A., Kellomäki, S., Strandman, H., & Venäläinen, A. (2010). Climate change impacts on forest fire potential in boreal conditions in Finland. *Climatic Change*, *103*(3), 383–398. https://doi.org/10.1007/s10584-009-9788-7

Kochanski, A. K., Mallia, D. V., Fearon, M. G., Mandel, J., Souri, A. H., & Brown, T. (2019). Modeling wildfire smoke feedback mechanisms using a coupled fire-atmosphere model with a radiatively active aerosol scheme. *Journal of Geophysical Research: Atmospheres*, *124*(16), 9099–9116. https://doi.org/10.1029/2019JD030558

Magalhães, N. D., Evangelista, H., Condom, T., Rabatel, A., & Ginot, P. (2019). Amazonian biomass burning enhances tropical Andean glaciers melting. *Scientific Reports*, *9*(1), 16914. https://doi.org/10.1038/s41598-019-53284-1

Marshall, S. J., & Miller, K. (2020). Seasonal and interannual variability of melt-season albedo at Haig Glacier, Canadian Rocky Mountains. *The Cryosphere*, *14*(10), 3249–3267. https://doi.org/10.5194/TC-14-3249-2020

McKendry, I. G., Christen, A., Lee, S. C., Ferrara, M., Strawbridge, K. B., O'Neill, N., & Black, A. (2019). Impacts of an intense wildfire smoke episode on surface radiation, energy and carbon fluxes in southwestern British Columbia, Canada. *Atmospheric Chemistry and Physics*, *19*(2), 835–846. https://doi.org/10.5194/acp-19-835-2019

Menounos, B., Hugonnet, R., Shean, D., Gardner, A., Howat, I., Berthier, E., et al. (2019). Heterogeneous changes in western North American glaciers linked to decadal variability in zonal wind strength. *Geophysical Research Letters*, *46*(1), 200–209. https://doi.org/10.1029/2018GL080942

Naz, B. S., Frans, C., Clarke, G., Burns, P., & Lettenmaier, D. P. (2014). Modeling the effect of glacier recession on streamflow response using a coupled glacio-hydrological model. *Hydrology and Earth System Sciences*, *18*, 787–802. https://doi.org/10.5194/hess-18-787-2014

Oerlemans, J., & Grisogono, B. (2002). Glacier winds and parameterisation of the related surface heat fluxes. *Tellus, Series A: Dynamic Meteorology and Oceanography*, *54*(5), 440–452. https://doi.org/10.1034/j.1600-0870.2002.201398.x

Pomeroy, J. W., Fang, X., & Ellis, C. (2012). Sensitivity of snowmelt hydrology in Marmot Creek, Alberta, to forest cover disturbance. *Hydrological Processes*, *26*(12), 1891–1904. https://doi.org/10.1002/hyp.9248

Pomeroy, J. W., Fang, X., & Marks, D. (2016). The cold rain-on-snow event of June 2013 in the Canadian Rockies—Characteristics and diagnosis. *Hydrological Processes*, *2914*, 2899–2914. https://doi.org/10.1002/hyp.10905

Pomeroy, J. W., Gray, D. M., Brown, T., Hedstrom, N., Quinton, W. L., Granger, R. J., & Carey, S. K. (2007). The cold regions hydrological model: A platform for basing process representation and model structure on physical evidence. *Hydrological Processes*, *2274*, 2650–2667. https://doi.org/10.1002/hyp.6787

Ryan, J. C., Hubbard, A., Stibal, M., Irvine-Fynn, T. D. L., Cook, J. M., Smith, L. C., et al. (2018). Dark zone of the Greenland Ice Sheet controlled by distributed biologically-active impurities. *Nature Communications*, *9*(1), 1065. https://doi.org/10.1038/s41467-018-03353-2

Sicart, J. E., Pomeroy, J. W., Essery, R. L. H., & Bewley, D. (2006). Incoming longwave radiation to melting snow: Observations, sensitivity and estimation in northern environments. *Hydrological Processes 2*, *20*(17), 3697–3708. https://doi.org/10.1002/hyp.6383

Skiles, S. M. K., Flanner, M., Cook, J. M., Dumont, M., & Painter, T. H. (2018). Radiative forcing by light-absorbing particles in snow. *Nature Climate Change*, *8*(11), 964–971. https://doi.org/10.1038/s41558-018-0296-5

Sokolik, I. N., Soja, A. J., DeMott, P. J., & Winker, D. (2019). Progress and challenges in quantifying wildfire smoke emissions, their properties, transport, and atmospheric impacts. *Journal of Geophysical Research: Atmospheres*, *124*(23), 13005–13025. https://doi.org/10.1029/2018JD029878

Stibal, M., Šabacká, M., & Žárský, J. (2012). Biological processes on glacier and ice sheet surfaces. *Nature Geoscience*, *5*(11), 771–774. https://doi.org/10.1038/ngeo1611

Stocks, B. J., Mason, J. A., Todd, J. B., Bosch, E. M., Wotton, B. M., Amiro, B. D., et al. (2003). Large forest fires in Canada, 1959–1997. *Journal of Geophysical Research*, *108*(1), 8149. https://doi.org/10.1029/2001jd000484

Stone, R. S., Anderson, G. P., Shettle, E. P., Andrews, E., Loukachine, K., Dutton, E. G., et al. (2008). Radiative impact of boreal smoke in the Arctic: Observed and modeled. *Journal of Geophysical Research*, *113*(14), 14–16. https://doi.org/10.1029/2007JD009657

Tedstone, A. J., Cook, J. M., Williamson, C., Hofer, S., McCutcheon, J., Irvine-Fynn, T. D. L., et al. (2019). Algal growth and weathering crust structure drive variability in Greenland Ice Sheet ice albedo. *The Cryosphere Discussions*, 1–24. https://doi.org/10.5194/tc-2019-131

Tennant, C., & Menounos, B. (2013). Glacier change of the Columbia Icefield, Canadian Rocky Mountains, 1919–2009. *Journal of Glaciology*, *59*(216), 671–686. https://doi.org/10.3189/2013JoG12J135

Tennant, C., Menounos, B., Wheate, R., & Clague, J. J. (2012). Area change of glaciers in the Canadian Rocky Mountains, 1919 to 2006. *The Cryosphere*, *6*(6), 1541–1552. https://doi.org/10.5194/tc-6-1541-2012

Versini, P. A., Velasco, M., Cabello, A., & Sempere-Torres, D. (2013). Hydrological impact of forest fires and climate change in a Mediterranean basin. *Natural Hazards*, *66*(2), 609–628. https://doi.org/10.1007/s11069-012-0503-z

Warren, S. G., & Wiscombe, W. J. (1980). A model for the spectral albedo of snow. II: Snow containing atmospheric aerosols. *Journal of the Atmospheric Sciences*, *37*(12), 2734–2745. https://doi.org/10.1175/1520-0469(1980)037<2734:AMFTSA>2.0.CO;2

Westerling, A. L., Hidalgo, H. G., Cayan, D. R., & Swetnam, T. W. (2006). Warming and earlier spring increase Western U.S. forest wildfire activity. *Science*, *313*(5789), 940–943. https://doi.org/10.1126/science.1128834

Williamson, S. N., & Menounos, B. (2021). The influence of forest fires aerosol and air temperature on glacier albedo, western North America. *Remote Sensing of Environment*, *267*, 112732. https://doi.org/10.1016/j.rse.2021.112732